Water Science & Technology

IWA PUBLISHING

Water Science & Technology Vol 84 No 9, 2194 doi: 10.2166/wst.2021.432

Investigation of the low impact development strategies for highly urbanized area via auto-calibrated Storm Water Management Model (SWMM)

Ömer Ekmekcioğlu [a,*], Muhammet Yılmaz [b], Mehmet Özger [a] and Fatih Tosunoğlu [b]

[a] Hydraulics Division, Civil Engineering Department, Istanbul Technical University, Maslak 34469, Istanbul, Turkey
[b] Department of Civil Engineering, Erzurum Technical University, 25050 Erzurum, Turkey
*Corresponding author. E-mail: omer.ekmekcioglu@itu.edu.tr

ÖE, 0000-0002-7144-2338; MY, 0000-0002-9844-6654; MÖ, 0000-0001-9812-9918; FT, 0000-0002-8423-1089

ABSTRACT

This study aims to investigate the effectiveness of the low impact development (LID) practices on sustainable urban flood storm water management. We applied three LID techniques, i.e. green roof, permeable pavements and bioretention cells, on a highly urbanized watershed in Istanbul, Turkey. The EPA-SWMM was used as a hydrologic-hydraulic model and the model calibration was performed by the well-known Parameter ESTimation (PEST) tool. The rainfall-runoff events occurred between 2012 and 2020. A sensitivity analysis on the parameter selection was applied to reduce the computational cost. The Nash-Sutcliffe efficiency coefficient (NSE) was used as the objective function and it was calculated as 0.809 in the model calibration. The simulations were conducted for six different return periods of a storm event, i.e. 2, 5, 10, 25, 50 and 100 years, in which the synthetic storm event hyetographs were produced by means of the alternating block method. The results revealed that the combination of green roof and permeable pavements have the major impact on both the peak flood reduction and runoff volume reduction compared to the single LIDs. The maximum runoff reduction percentage was obtained as 56.02% for a 10 years return period of a storm event in the combination scenario.

Key words: automatic calibration, low impact development, PEST, sensitivity analysis, SWMM, urban floods

HIGHLIGHTS

- The PEST software is used for the auto-calibration of US EPA-SWMM and the calibration results are statistically significant.
- The green roof application has more impact on both the peak discharge reduction and the volume reduction than both the permeable pavements and bioretention cells in the highly urbanized Ayamama watershed.
- The combination of green roof and permeable pavements has substantial effect on flood mitigation.

1. INTRODUCTION

Urbanization and growing population have increased the significance of a sustainable utilization of water resources, particularly in rapidly developing urban areas (Koc & Işık 2020; Ekmekcioğlu *et al.* 2021). An increase in impermeable areas with the effect of urbanization reduces the storm water infiltration. This results in a higher volume of surface runoff, frequency of floods, and so, shorter peak flow lag times (Abi Aad *et al.* 2010; Qin *et al.* 2013; Peng & Stovin 2017; Liew *et al.* 2021). Thus, an increasing imperviousness due to the urbanization brings significant changes in the land use and alterations of hydrological cycles (Palla & Gnecco 2015). In particular, intense storm events have serious impacts on the society by various damages to the environment as well as population displacement and causing casualties. In this direction, several flood mitigation strategies, such as structural measures, low impact development (LID) practices and conventional approaches, are proposed by the research society. The LID strategies have been proposed and adopted to mitigate the impact of urbanization. The principle of LID practices is the attempt to control flow through decentralized, small-scale resource control and to bring the development space close to the natural hydrological cycle model as much as possible. LID applications can reduce flooding and improve ecological conditions by providing storage, rainfall retention, runoff detention and infiltration facilities (Peng & Stovin 2017; Bai *et al.* 2018; Cristiano *et al.* 2021). Among the LIDs, green roofs, rain barrels, rain gardens, bioretention cells and permeable pavements are the most commonly used solutions. However, determining the most suitable type of LID

practices to be chosen for a study area is delicate, since the selection and positioning of LID controls can be abundant due to varying features of watersheds. Thus, characteristics of the development site and considering the maximum reductions of runoff with minimum costs are essential (Cano & Barkdoll 2017). Moreover, studies over the past two decades have provided significant improvement in applying such techniques and it is generally accepted that adopting a combination of LIDs is more effective than a single LID in surface runoff reduction (Guan *et al.* 2015). For the reasons mentioned above (especially basin characteristics), this study evaluates not only the single LID controls (green roofs, permeable pavements and bioretention cells), but also their combinations to reduce the imperviousness effect for a highly urbanized watershed.

Accurate modeling of hydrological process like storm water flow volume can provide important information on urban planning, flood control and water resources management. Hence, many computer-based models have been developed to constitute the hydrological process and estimate the urban flow, i.e. RORB, MOUSE, WBNM (watershed bounded network model), HEC-HMS and Storm Water Management Model (SWMM). Among the various models developed in the literature, SWMM appears to be the most commonly used model to conduct the hydrological simulations in urban areas with several LID alternatives (Masseroni & Cislaghi 2016; Abualfaraj *et al.* 2018; Rodrigues *et al.* 2021). SWMM can effectively be used to simulate the hydrologic response of an urban watershed as well as to assess the capabilities of various LID controls.

Depending on the complexity, a hydrological model contains several parameters. Therefore, the parameter optimization is an essential step (Eckart *et al.* 2018). However, estimation of model parameters is usually hard, due to the extensive uncertainties such as model structure, type of parameters, initial conditions and parameter values that are measured directly in the field (Liu & Gupta 2007). For this reason, model calibration becomes a key aspect to improve the model accuracy. The conventional model calibration procedure (manual calibration) has been performed by means of trial and error approach in early studies (Chung *et al.* 2011). Afterwards, computer-based automated calibration techniques become increasingly popular because of the time-consuming nature and subjectivity of manual calibration strategies. Shahed Behrouz *et al.* (2020) proposed a new tool for the auto-calibration of SWMM parameters, OSTRICH-SWMM, to reduce the computational effort. Also, Perin *et al.* (2020) developed an auto-calibrated SWMM package with the integration of Parameter ESTimation (PEST) tool. In this paper, PEST is integrated into EPA-SWMM to perform the calibration process as it is one of the prominent and open source optimization tools (PEST n.d.). PEST is considerably useful since no programming is required to calibrate a model owing to fact that the model has its own input and output files (Doherty 2018).

A few of the similar studies using SWMM in hydrological models are summarized in Table 1. Fassman & Blackbourn (2010) tested an interlocking block permeable pavement site to investigate the impacts of LIDs on peak runoff. They found that all permeable pavement designs are highly effective in flood reduction during rainfall events. Qin *et al.* (2013) used SWMM for simulation of runoff in addition to the performance of LID applications, such as swale, permeable pavement and green roof, under different rainfall characteristics in an urbanized basin in China. They showed that all three LID designs are highly effective in flood reduction during both the heavier and shorter rainfall events. Liao *et al.* (2014) provided comparisons for cost–effectiveness analyses and flood reduction on different LID practices in highly urbanized regions. They concluded that the combination of bio-retention and infiltration trench showed satisfactory performance in flooded and floodplain areas. Masseroni & Cislaghi (2016) used an automatic optimization method (the 'fmincon' function) for calibration of the SWMM. Also, they modelled the hydrologic effect of the green roof scenarios at the catchment scale and presented that the total runoff volume and the peak runoff rate reduced by 35% and 30, respectively. Ahmed *et al.* (2017) implemented different LID strategies to the urban catchment of a university campus in Malaysia to investigate the impacts of LIDs on peak runoff. They not only showed that infiltration trench designs can be effective for reducing peak flow but also indicated the optimum physical parameter values for the utilized particular LID types. Zhang *et al.* (2018) examined the effect of the initial groundwater table depth on LID simulations together with the different rainfall patterns and soil types. They concluded that the rainfall types and in-situ soils have less impact on the LID performance in shallow groundwater tables compared to deeper groundwater tables. Also, they found that shallow groundwater tables are more effective than the shallower groundwater tables, particularly for the storm events that have relatively higher intensity and longer duration. Thus, incorporating the groundwater tables' influence in SWMM leads to more accurate results than the conventional SWMM for the LID practices. Hamouz & Muthanna (2019) optimized the six green roof and grey roof practices with 1-minute resolution data and then considered the impact of the snow melting process on LID applications. They showed that inclusion of snow melting reduces the LID performance in both the calibration and the validation periods, especially in the winter season.

To the best of the authors' knowledge, there are only a few published studies in the literature related to the application of automatic calibration coupled with SWMM together with evaluating the performance of LIDs (Masseroni & Cislaghi 2016;

Table 1 | Review of the EPA-SWMM related studies

References	Study location	Area (ha)	Optimization type	LID type and implemented area (%)	Sensitivity analysis	Calibrated parameters (in case of automatic optimization)
Qin *et al.* (2013)	Southwest of Guang-Ming, New District, China	600	Manual	Swale (10%), Green roof (15%) Permeable pavements (22%)	Yes	–
Burszta-Adamiak & Mrowiec, (2013)	The University of Environmental and Life Sciences, Poland.	N/A	Manual	Green roof	No	–
Palla & Gnecco (2015)	Colle Ometti, Italy	5.5	Manual	Green roof (31%) Permeable pavements (16%)	Yes	–
Guan *et al.* (2015)	Espoo, Southern Finland	12.3	Manual	Rain barrel (10.2%) Porous pavement (10.5%)	Yes	–
Masseroni & Cislaghi (2016)	Seveso Basin, Italy	2,500,000	Automatic (Fmincon Function)	Green roof (36%)	No	Stor_perv, Stor_imperv,N-Perv, N-Imperv,decay
Zhang *et al.* (2018)	Central Kitsap County Campus, Washington, United States	2.63	Automatic (Genetic Algorithm)	Porous pavement (35%) Bioretention cell (9 cells)	No	Roughness, conductivity, suction head, Stor_perv, N-Perv
Hamouz & Muthanna (2019)	Coastal Area of Trondheim, Norway	0.1	Automatic (Shuffle Complex Evolution)	Green roof (88%) Grey roof (88%)	Yes	Porosity, field capacity, conductivity, conductivity slope, void fraction, Manning's n
Shahed Behrouz *et al.* (2020)	Buffalo, United States	104.1	Automatic (Ostrich)	N/A	Yes	Roughness, N-Imperv, imperviousness (%), conductivity, Stor_perv, InitDef, Width
Perin *et al.* (2020)	Galleriano Di Lestizza, Italy	36	Automatic (PEST)	N/A	Yes	Imperviousness (%), width, slope, roughness, initial abstraction

Hydrological parameter: Stor_perv is depth of depression storage on the pervious area, Stor_imperv is depth of depression storage on the impervious area; N-Perv is Manning for pervious area; N-Imperv is Manning for impervious area; decay is decay constant for the Horton infiltration curve; Roughness is Manning's roughness coefficient; Conductivity is hydraulic conductivity; Porosity is a measure of the void; Width is the width of overland flow path in a subcatchment; Slope is the slope of a subcatchment; InitDef is Initial soil moisture deficit for Green-Ampt infiltration.

Zhang *et al.* 2018; Hamouz & Muthanna 2019). In addition, several researches exist utilizing the SWMM to perform the hydrological modelling of urbanized areas in Turkey (Gülbaz & Kazezyılmaz-Alhan 2017; Gülbaz *et al.* 2019). However, both the LID design and the automatic calibration coupled with SWMM have not yet been considered in Turkey so far. Hence, the main objectives of this study are: (1) to determine the sensitive parameters of SWMM by using PEST; (2) to calibrate the SWMM's sensitive parameters by adopting PEST; (3) to analyze the runoff reduction efficiency of three stand-alone LID techniques (green roof, permeable pavements and bioretention cells) and combinations of them for the densely populated urbanized watershed; (4) to identify the optimal design by assessing the hydrological performance of the different designs of LID practices for peak flow and volume reduction; (5) to evaluate the impact of the rainfall intensity on the hydrologic response under the synthetic hyetographs derived for different return periods; that is, 2, 5 10, 25, 50 and 100 years.

2. MATERIALS AND METHODS

2.1. Study area

This study was conducted for the Ayamama watershed, which is located in the European part of Istanbul, Turkey. The watershed extends between 28° 21′ 18″E and 28° 24′ 43″E longitudes and between 40° 58′ 14″N and 41° 08′ 12″N latitudes (Nigussie & Altunkaynak 2016). The Ayamama stream has a 42 km length in total including the main stream (22 km) and five tributaries (20 km) (Figure 1). Istanbul has 39 districts and the Ayamama stream runs through six different densely populated districts (Ekmekcioğlu *et al.* 2020). The entire watershed of the river covers nearly a total area of 75 km^2 and contains various land use types. The watershed has undergone various change in terms of the land use from the 1990s till today; such that, from 1987 to 2013, the percentage of built-up area has increased from 23% to 62%. However, the urbanization and unstudied structuring led to an increase in surface runoff and a number of flash floods. For instance, the flood event that occurred in 2009, 9 September, resulted in an extensive loss of property and even worse, 31 casualties. On that day, a daily rainfall amount had been recorded as 175.2 mm (correspond to the nearly 100-year return period rainfall event for the Ayamama watershed) at Olimpiyat Station, which is also used in this study. After this unfortunate event, the recreational areas were built around the river. The Ayamama stream was also remediated; such that the cross-section and floodplain of the river were extended. In this study, we focus on the hydrological rainfall-runoff process in Ayamama watershed by considering the current cross-section, storm water infrastructure and the up-to-date basin properties.

2.2. Data used

EPA-SWMM utilizes meteorological data, such as precipitation and temperature, to simulate the hydrological process. Temperature data is used in the calculation of evaporation (Rossman 2015). The meteorological data was obtained from the Istanbul Metropolitan Municipality Disaster Coordination Center (AKOM 2020). The precipitation and temperature data are recorded at 1-minute intervals (Station Name: Olimpiyat station, Station ID: 20022, 41°05′05.7″N; 28°45′58.3″E). Also, we obtained the runoff data (in terms of flow depth) from AKOM as it is recorded at 1-minute intervals as well. The location of the streamflow gauge station is shown in Figure 1 with a red triangular symbol. The recorded flow depth data was used to validate the EPA-SWMM simulation results. To delineate the watershed boundaries, we utilized the digital terrain

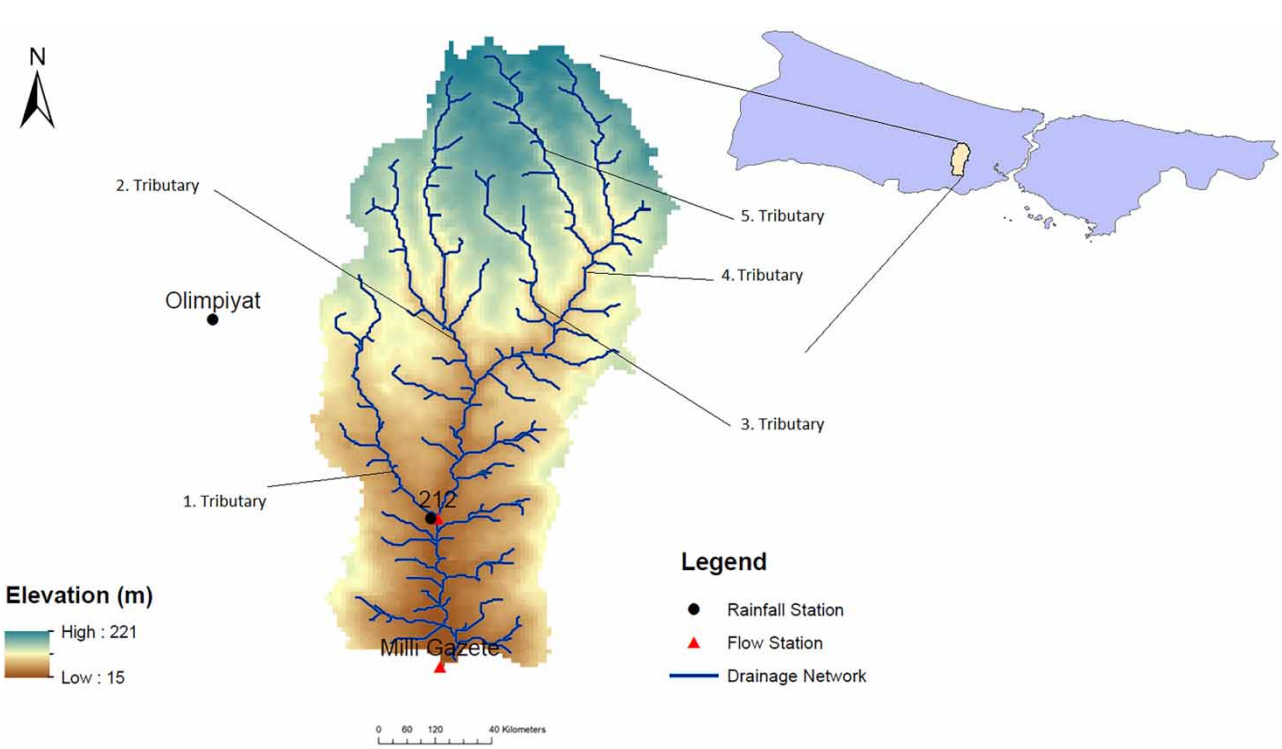

Figure 1 | Study area.

elevation data (30 m×30 m resolution) which was produced by Istanbul Metropolitan Municipality Water and Sewerage Administration (ISKI 2020). Storm water pipe network and channels, the locations and dimensions of ponds, ditches and culverts were also obtained from ISKI to identify the outlet of each sub-watershed. Land cover/land use data was obtained from the CORINE Land Cover Data (Copernicus Europe's eye on Earth and Land Monitoring Service 2020) and analytical surveys of the Istanbul project (BIMTAS 2020).

2.3. Description of EPA SWMM

The EPA Storm Water Management Model (SWMM) was first introduced in 1971. SWMM has been employed by a great deal of researchers for planning, analysis and design of stormwater runoff, combined sewers, sanitary sewers, and other drainage systems in urban areas. SWMM, being a dynamic hydrology-hydraulic model, is a suitable tool for single event or long-term simulation of runoff quantity and quality, particularly for urban areas. Also, SWMM has many advantages in solving different types of water-related problems in urban areas, especially in the cases of open channels from the surface and where underground pipes are complex as well as a runoff quantity is to be simulated. It is worth mentioning that EPA-SWMM is limited to 1D simulations and is not able to perform analysis of surface flow for a particular area (Yin *et al.* 2020; Koc *et al.* 2021). In this study, the EPA-SWMM version 5.1 (launched in 2015) was utilized.

In SWMM, infiltration losses are calculated by using five methods; namely Horton, modified Horton, Green-Ampt, modified Green-Ampt and curve number (CN). The model employs each sub-basin as a nonlinear reservoir runoff model and calculates the surface runoff on each sub-basin by simultaneously solving the continuity equation and Manning equation given below as Equations (1) and (2), respectively. In this study, we described each sub-basin as a piece of land consisting of pervious and impervious areas that convey the runoff to an outlet point, which may be a node of the drainage network or another sub-basin.

$$\frac{dV}{dt} = (A \times i_k) - Q \tag{1}$$

$$Q = W \times \frac{1.49}{n} \times (D - D_i)^{5/3} \times S^{1/2} \tag{2}$$

where V represents volume of water over the sub-basin; A is the sub-basin area; i_k is net rain; Q is the sub-basin outflow; n is Manning's roughness coefficient; W is the width of basin overland flow; D is the depth of water on the sub-basin; D_i is depth of the surface depression storage; S is the slope of the sub-basin.

SWMM utilizes the conservation of mass and momentum equations, known as the Saint-Venant equations, for flow routing. SWMM offers three options: (*i*) steady flow, (*ii*) kinematic wave, and (*iii*) dynamic wave routing (Rossman 2015; Hossain *et al.* 2019). The dynamic wave routing model solves the one-dimensional continuity equation and full momentum equation presented in Equations (3) and (4), respectively:

$$\frac{\partial A}{\partial t} + \frac{\partial Q}{\partial x} = 0 \tag{3}$$

$$\frac{1}{g}\frac{\partial V}{\partial t} + \frac{V}{g}\frac{\partial V}{\partial x} + \frac{\partial y}{\partial x} + S_f - S_0 = 0 \tag{4}$$

in which, Q is the flow in the conduit; A and x represent the area of the flow cross-section and longitudinal distance, respectively (Li *et al.* 2016).

In the momentum equation., $1/g\,\partial V/\partial t$, $V/g\partial V/\partial x$, $\partial y/\partial x$, S_f and S_0 are identified as local acceleration, convective acceleration, pressure force, friction slope and channel slope, respectively. Kinematic wave routing model is obtained by neglecting local and convective acceleration, as well as pressure force in the momentum equation. The SWMM solves not only the continuity equation for each node in the model but also the momentum equation throughout the conduit connections (Hossain *et al.* 2019). The dynamic wave routing model was used in this study since it provides the most theoretically consistent results.

2.4. Objective function and statistical indices

There are several efficiency criteria for the evaluation of hydrological model performance. In this paper, the Nash-Sutcliffe efficiency (*NSE*) (Nash & Sutcliffe 1970) was chosen for streamflow performance as it is one of the most commonly

used performance metrics in hydrological applications (Biondi *et al.* 2012; Hamouz & Muthanna 2019). NSE is given in Equation (5):

$$NSE = 1 - \frac{\sum_{i=1}^{n} (O_i - P_i)^2}{(O_i - \bar{O})^2} \tag{5}$$

where O_i represents the observed water depth, P_i is the simulated water depth, $\bar{O}$ is the average of observed values, and n is the number of samples. The range of NSE varies between $-\infty$ and 1. The value of $NSE = 1$ indicates a perfect match between simulated and observed discharge.

In addition to the NSE, the calibration results were assessed in terms of different statistical indices; that is, root mean square error (RMSE), performance index (PI), Wilmott's refined index (WI) and relative error (RE). Even though these indices are generally used in the evaluation of the mathematical modeling studies, we intended to demonstrate whether calibration strategy is robust and the obtained results are statistically significant. The equations of the performance indicators are as follows:

$$RMSE = \sqrt{\frac{1}{n}\sum_{i=1}^{n} (P_i - O_i)^2} \tag{6}$$

$$PI = \frac{\frac{RMSE}{\overline{O_i}}}{1 + \frac{\sum_{i=1}^{n} [(O_i - \overline{O_i})(P_i - \overline{P_i})]}{\sqrt{\sum_{i=1}^{n} (O_i - \overline{O_i})^2 \sum_{i=1}^{n} (P_i - \overline{P_i})^2}}} \tag{7}$$

$$WI = 1 - \frac{\sum_{i=1}^{n} |P_i - O_i|}{c \times \sum_{i=1}^{n} |O_i - \overline{O_i}|}, \text{ when } \sum_{i=1}^{n} |P_i - O_i| \leq c \times \sum_{i=1}^{n} |O_i - \overline{O_i}| ; \text{ (with } c = 2) \tag{8a}$$

$$WI = \frac{c \times \sum_{i=1}^{n} |O_i - \overline{O_i}|}{\sum_{i=1}^{n} |P_i - O_i|} - 1, \text{ when } \sum_{i=1}^{n} |P_i - O_i| > c \times \sum_{i=1}^{n} |O_i - \overline{O_i}| ; \text{ (with } c = 2) \tag{8b}$$

$$RE = \frac{|O_i - P_i|}{O_i} \tag{9}$$

in which, $\overline{O_i}$ and $\overline{P_i}$ are the average of observed and simulated values, respectively. The WI varies between -1 and 1 (Willmott *et al.* 2012), while the PI varies between 0 and ∞ (Gandomi & Roke 2015). Lower RMSE and RE value indicates a good-match between observed and simulated values.

2.5. Sensitivity analysis and parameter optimization

Sensitivity analysis is performed to identify the optimum number of parameters for model calibration and to determine the most appropriate calculation time step combination for both simulation results and run-time (Krebs *et al.* 2013). Before the model calibration, the most influential parameters on calibration performance are determined using the sensitivity analysis, and then the sensitive parameters are included in a subsequent model calibration. The PEST provides a sensitivity analysis module by adjusting the model inputs during the optimization process, changing the parameter values, reading the outputs of interest, saving their values, and restarting the calculation cycle (Liu *et al.* 2005). Parameters determined for sensitivity analysis and assigned parameter intervals are shown in Table 2. Note that the parameter ranges were obtained from the EPA-Storm Water Management Model Manual (Rossman 2015).

Table 2 | Selected calibration parameters and assigned parameter ranges

Category	Parameter name	Description	Surface type	Range
Sub-catchment	N-Imperv	Manning for impervious area	Asphalt/Concrete	0.002–0.019
	N-Perv	Manning for pervious area	Grass/tree	0.002–0.019
	pctzero	Percent of impervious area with no depression storage (%)	–	0–100
Infiltration	maxrate	Maximum rate on the Horton infiltration curve (mm/hr)	Infiltration model	0.6–5
	minrate	Minimum rate on the Horton infiltration curve (mm/hr)	Infiltration model	0.254–1.2
	decay	Decay constant for the Horton infiltration curve (1/hr)	Infiltration model	2–7
	drytime	Time for a fully saturated soil to completely dry (days)	Infiltration model	2–14
Conduit	roughness	Manning's roughness coefficient	Concrete/PVC	0.04–0.14

The EPA-SWMM rainfall-runoff model is automatically calibrated by using the well-known PEST tool. PEST is a nonlinear parameter estimation and optimization tool offering model independent optimization routines (Liu *et al.* 2005). To start the optimization process, PEST requires to generate three files: (*i*) PEST instruction file (identifying model output variables); (*ii*) PEST template file (identifying model parameters); and (*iii*) PEST control file (supplying all necessary information for PEST). PEST control file is the most significant file among these three files, since it contains calibration data, initial values, upper and lower boundaries of the possibly calibrated parameters, maximum number of runs, and also as a stop rule, the value of the maximum relative objective function change (Liu *et al.* 2005). During the automatic calibration process, the PEST takes control of the EPA-SWMM model and runs the model many times to determine the optimized values within the assigned lower and upper limits until the specified stop criterion is reached.

The PEST uses a number of different criteria to determine when to stop this recursive process: (*i*) the value of the maximum relative objective function change, (*ii*) exceeding the maximum number of runs, (*iii*) convergence of adjustable parameters to optimal values; (*iv*) insignificant relative parameter change relative to the successive iterations. The deviations between model output and observed flow rates are calculated as follows:

$$\emptyset = \sum_{i=1}^{n} w_i [r_i - r_i']^2 \tag{10}$$

where $\emptyset$ represents the objective function, n indicates the number of total observations, w_i refers to the weight of the ith observation, r_i and r_i' are the observed and simulated flow for the ith observation, respectively.

2.6. Low impact development strategies

EPA-SWMM provides a user-friendly module to conduct the green infrastructural practices. In this way, controlling site runoff is achieved through using the low impact development (LID) strategies; that is, rain gardens, bioretention cells, infiltration trenches, green roofs, permeable pavements, and so on. One can increase the infiltration and evaporation as well as reduce the surface runoff by capturing the direct rainfall via LID practices. In the EPA-SWMM LID toolbox, LID controls are assigned to a user-defined sub-watershed (Taji & Regulwar 2019). Unit area basis vertical layers exist for each LID type and the parametrization of these layers is performed according to the site condition and LID design standards. In this study, green roof, permeable pavement and bioretention cells were applied as stand-alone green infrastructure practices, while a combination of the best performed LID options was adopted as well.

The green roof structure comprises three layers: (1) Surface Layer, (2) Soil Layer and (3) Drainage Layer. Green roofs are set based on the similar technique with the bioretention cell; however, a porous or conveying layer is also included to discharging the water from the roofs. We used the green roof LID type since there was limited open space in the selected study area. The green roof application is effective in particularly urbanized areas and widely distributed industrial places (Platz *et al.* 2020). In addition to the type of the buildings, the age of the buildings is another major challenge in LID applications. Therefore, we identified the deployed green roof areas in this regard.

Another LID type used in this study is the permeable pavement, which is an instrumental alternative for conventional pavements. Permeable pavements consist of four layers: (1) Surface Layer, (2) Pavement Layer, (3) Storage Layer and (4) Underdrain Layer. Installing permeable pavements leads to the conversion of rainfall to two different outflows, which are

the surface outflow and the drain outflow. Also, an infiltration occurs due to the underdrain layer and the drain outflow already contains some amount of infiltration (Zhang & Guo 2014). The last LID practice used within the scope of the study is the bioretention cell, which is defined as a landscape depression. The bioretention cell consists of four layers: (1) Surface Layer, (2) Soil Layer, (3) Storage Layer, and (4) Underdrain Layer (Rodrigues *et al.* 2021; Tirpak *et al.* 2021). It is widely implemented to capture storm water runoff from external impermeable basins to reduce surface pollutant loads, runoff volumes, and peak flow rates (Liu & Fassman-Beck 2017; Rycewicz-Borecki *et al.* 2017). The bioretention cells also provide many benefits such as aesthetic enhancement and ecological restoration (Houdeshel *et al.* 2012; Demuzere *et al.* 2014).

Moreover, there are two ways for the application of the combined LID practices. First option is to divide the entire watershed into several sub-watersheds that contain one type of LID, while the second option is the deployment of the combined LID techniques in a smaller number of sub-watersheds (Men *et al.* 2020). It is worth mentioning that the latter is suitable for larger study areas. Since the Ayamama watershed covers an extensive surface area and multiple land use types; in this research, applying the combination scenario was considered. The assumed parameter values for LIDs presented are in Table 3.

3. MODEL DEVELOPMENT

In this study, Ayamama watershed, which is one of the most densely urbanized areas in Istanbul metropolitan city, was investigated. The reason behind the selection of this area is because of its strategic location, such that the Ayamama watershed hosts several industrial, commercial and residential areas as well as airport and university campuses. There are two different points located for the runoff measurement on the Ayamama stream; that is, 212-AVM station and Milli Gazete station, however the Milli Gazete gauge was chosen as an outfall since it is the closest point to the river outlet. Therefore, the watershed delineation was performed according to the Milli Gazete station. After that, the US EPA-SWMM model was configured to constitute the hydrologic-hydraulic process. First, the sensitivity analysis was carried out and second, automatic calibration was performed by means of PEST. Next, the model validation was performed considering the precipitation and streamflow values recorded in the 212-AVM station. After validation, three different LID practices were determined; that is, green roof, permeable pavement and bioretention cells, to apply on the sub-watersheds considering the characteristics of each. At last,

Table 3 | LIDs characteristics and the parameter values

Control name Layer	Property	Green roof Value	Permeable pavement Value	Bioretention cell Value	Source for value selection
Surface Layer	Berm height (mm)	25	0	150	[a]
	Vegetation volume fraction	0.1	0	0.1	[a] and [c]
	Surface roughness (n Manning)	0.03	0.01	0.1	[a] and [b]
	Surface slope (%)	1	0	0	[a]
Soil Layer	Thickness (mm)	150	–	200	[a]
	Porosity (volume fraction)	0.5	–	0.5	[a]
Pavement Layer	Thickness (mm)	–	150	–	[a]
	Void ratio (voids/solids)	–	0.4	–	[a]
	Impervious surface (fraction)	–	0.3	–	[a]
	Permeability (mm/h)	–	72	–	[a]
Storage Layer	Thickness (mm)	–	300	500	[a]
	Void ratio (voids/solids)	–	0.4	0.75	[a]
	Seepage rate (mm/h)	–	750	750	[a]
Drainage Mat Layer	Thickness (mm)	75	–	–	[a]
	Void fraction (voids/solids)	0.5	–	–	[a] and [c]
	Roughness (n Manning)	0.1	–	–	[a] and [c]
Underdrain Layer	Underdrain diameter (mm)	–	100	100	[d]

Data source
[a]Rodrigues *et al.* (2021).
[b]Abualfaraj *et al.* (2018).
[c]Hamouz & Muthanna (2019).
[d]Tirpak *et al.* (2021).

the hydrographs (time series of water depth at outlet) were obtained for each LID scenario and the volume reduction and peak runoff reduction rates were calculated to evaluate whether the adopted runoff reduction strategies are effective on the surface flow. Figure 2 illustrates the framework of the current study.

3.1. Watershed delineation and SWMM setup

The study area is divided into 41 sub-watersheds based on the land use, stormwater pipe network and digital elevation model and the watershed area was calculated as approximately 45 km². The watershed delineation was performed by means of the commercial software; that is, Watershed Modelling System (WMS), and the properties of each sub-watershed were defined in SWMM. Table 4 shows the area, imperviousness percentage and average slope values of each watershed; however, it is worth

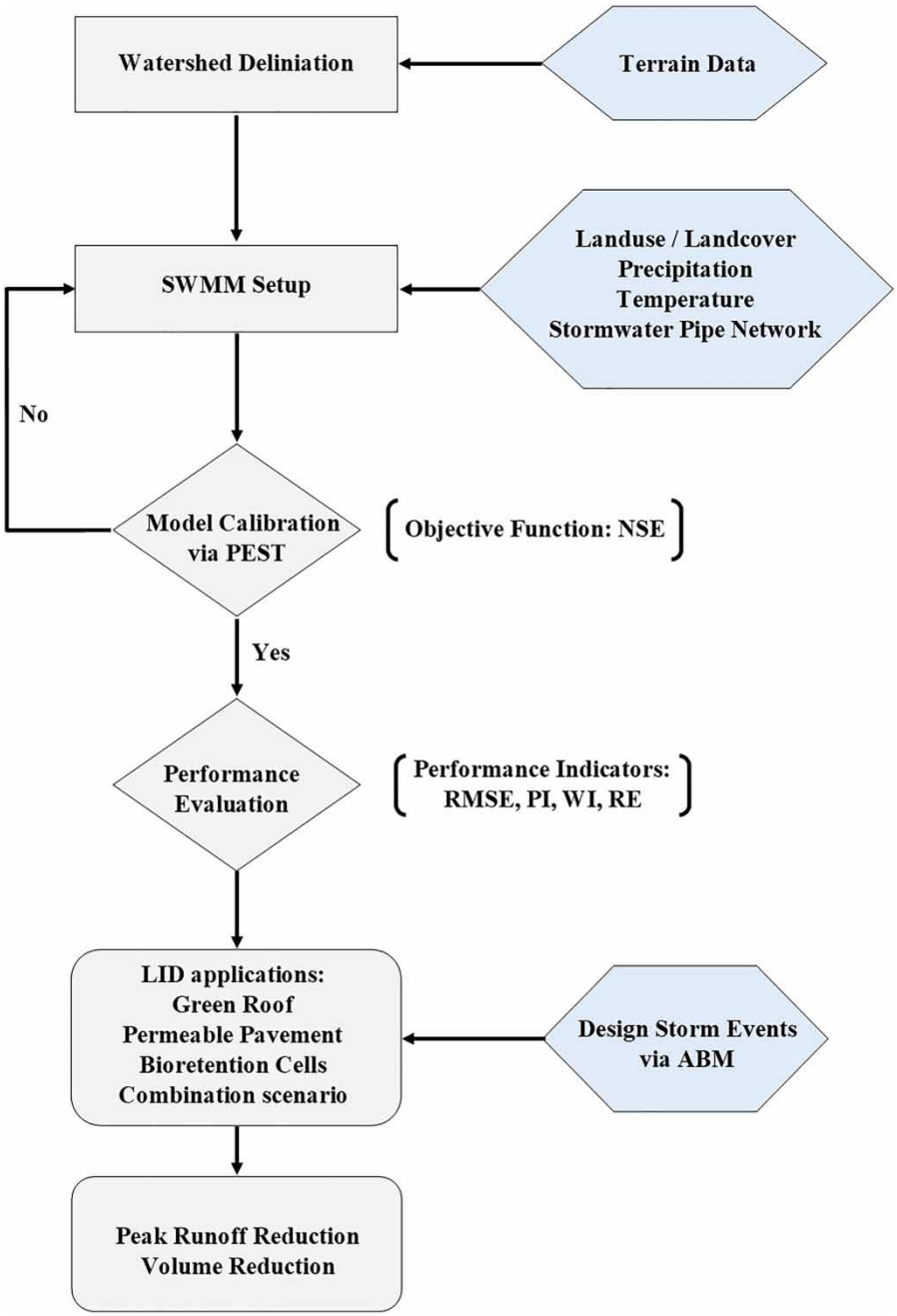

Figure 2 | Framework of the study.

Table 4 | The sub-watershed properties of entire Ayamama watershed

No.	Area (ha)	Slope (%)	Imperviousness (%)	No.	Area (ha)	Slope (%)	Imperviousness (%)
1	489	9.64	15.6	**22**	73	6.16	81
2	446	11.21	7.64	**23**	80	6.55	73.25
3	113	7.4	40.78	**24**	38	7.71	78.68
4	596	6.5	24.26	**25**	31	10.14	74.68
5	128	7.5	24.17	**26**	52	7.68	71.92
6	205	10.42	41.82	**27**	52	9.81	65
7	336	9.45	7.03	**28**	69	9.28	79.49
8	189	10.02	1.5	**29**	175	8.44	63.86
9	85	10.64	59.11	**30**	33	10.17	68.64
10	51	10.88	73.24	**31**	37	7.48	49.86
11	60	10.09	80	**32**	66	9.57	48.33
12	21	9.68	77.3	**33**	205	9.23	71.44
13	64	14.15	48.28	**34**	43	8.97	59.88
14	146	10.48	39.97	**35**	69	8.47	75.36
15	145	8.2	1.75	**36**	73	6.22	83.63
16	193	7.5	15.57	**37**	65	8.14	81.31
17	35	7.8	85	**38**	108	9.27	75.37
18	345	7.69	80	**39**	40	7.12	71
19	92	7.39	85	**40**	135	8.49	60
20	134	9.33	85	**41**	27	8.1	70.19
21	152	8.62	70				

mentioning that the rest of the properties (or SWMM parameters) of each element, such as maxrate, minrate and roughness, were obtained by automatic calibration.

As can be seen from Table 4, the watershed areas vary between 21 ha and 596 ha. The minimum slope was observed in Watershed #22, while the maximum slope was observed in Watershed #13 as 6.16% and 14.15%, respectively. In addition, we determined the percentage of imperviousness for each sub-watershed according to the CORINE Land Cover satellite database (Copernicus Europe's Eye on Earth & Land Monitoring Service 2020). The average imperviousness was calculated as 57.7% for the entire watershed. Also, nearly 70% of the number of sub-watersheds have more than 50% imperviousness. It indicates that the LID practices are not only applicable but also have considerable effect on the surface runoff.

The grey dashed lines represent the sub-watersheds borders in Figure 3(a), while the black solid lines and the red triangle illustrate the conduits and outfall in Figure 3(b), respectively. Figure 3(c) shows the implemented LID areas within the scope of this study while Figure 3(d) shows the Landcover data covered by the study area. In addition to the 41 sub-watersheds, there are 133 conduits in the entire watershed. The conduits were determined based on the stormwater drainage network and the main channel of the Ayamama River. The detailed information; that is, the top and bottom levels, collectors, cross-sections etc., about the drainage network and the main channel, was collected from the ISKI. For the flow routing through the conduits, the dynamic wave routing method was used to solve the Saint-Venant equation since it is suitable for non-uniform and unsteady flow conditions in addition to the abilities of accounting channel storage and backwater effects (Eckart *et al.* 2018). Based on the recommended intervals in the literature given for the materials used in the stormwater drainage network and the main cross-section of the river, the Manning's roughness coefficient values were optimized for each conduit by using PEST. Also, we utilized the Horton's infiltration method as it better represents the infiltration capacity curve than the other methods, such as the SCS-CN and the Green-Ampt method. The parameters of Horton's method were optimized via the PEST algorithm to determine the best match with the watershed conditions (Hossain *et al.* 2019).

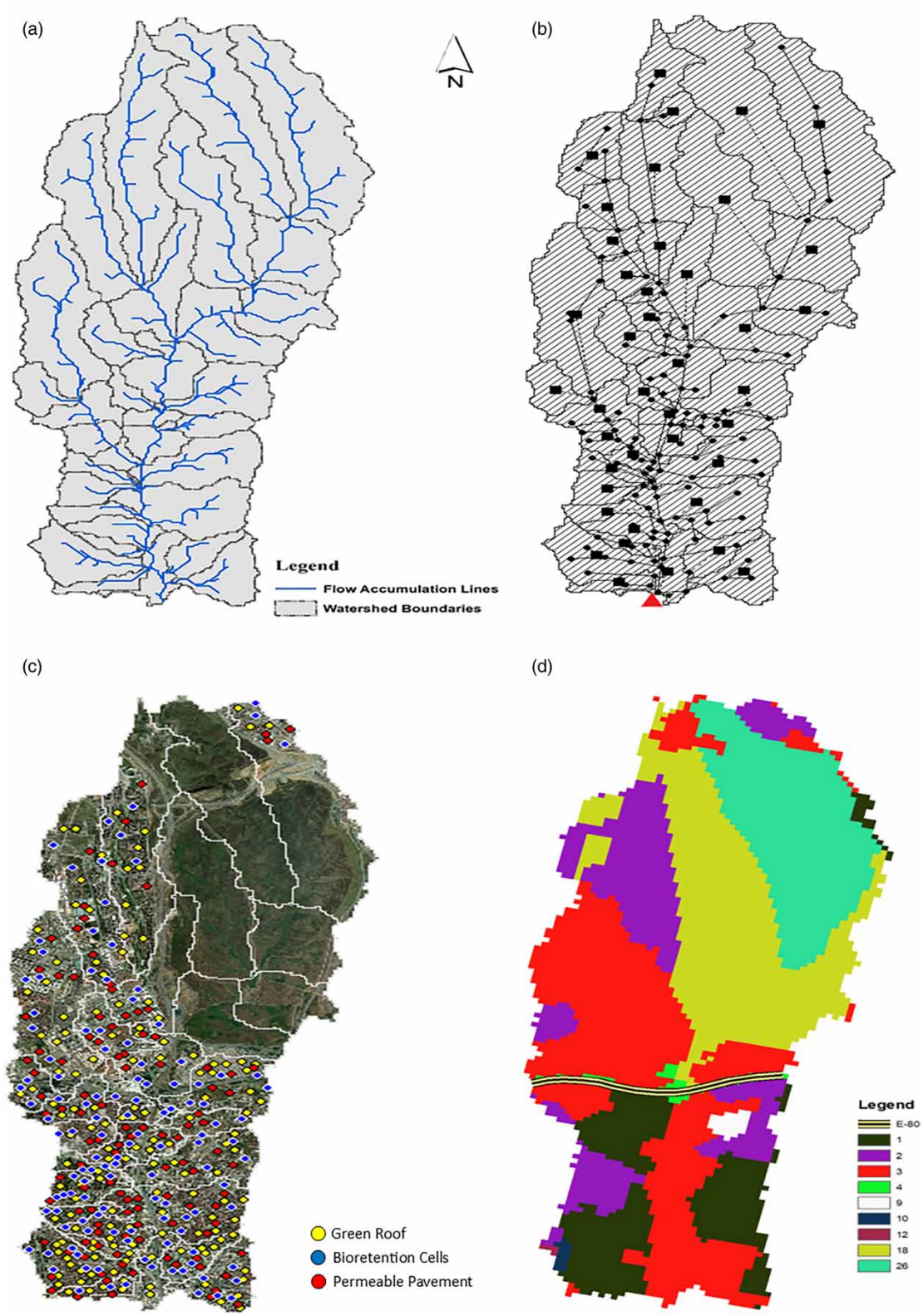

Figure 3 | Delineated sub-watersheds and other components of the hydraulics in SWMM framework. (a) Sub-watersheds and flow accumulation lines, (b) nodes and conduits, (c) implemented areas for LID practices, (d) Landcover (1: Continuous urban fabric, 2: Discontinuous urban fabric, 3: Industrial or commercial units, 4: Road and rail networks and associated land, 9: Construction sites, 10: Green urban areas, 12: Non-irrigated arable land, 18: Pastures, 26: Natural grasslands).

3.2. Low impact development implementation

In this study, three different stand-alone LID techniques; that is, green roof, permeable pavement, and bioretention cells, are applied to a highly urbanized area located in the European part of the Istanbul; that is, the Ayamama watershed. Firstly, suitable areas for the application of the LID practices were determined via aerial photographs, such that 8.90%,6.85% and 8.1% (depending on the sub-watershed properties) of the entire Ayamama watershed are available for green roofs, permeable pavements and bioretention cells, respectively. It is important to note that the applicable area of the green roof technique is larger than the permeable pavement as the study area consists of several industrial facilities and various structural types. Also, all the restrictions on the construction of three LID techniques were considered. For instance, a great deal of aged buildings exist in the Ayamama watershed; such that this is a handicap for positioning the green roofs. There is also the E-80 highway, which is quite close to the Ayamama stream, and the E-80 highway is not included in the possible permeable pavement areas due to the fact that the heavy traffic leads to serious construction difficulties. Also, similar factors regarding the implementation challenges were pursued in the identification of potential areas to apply bioretention cells. Secondly, the stand-alone LID practices were applied to the auto-calibrated SWMM model and the simulations were conducted by considering six different storm-event scenarios, i.e. 2, 5, 10, 25, 50 and 100-year return periods. The alternating block method (ABM), which introduces a simple way to develop a storm profile from Intensity-Duration-Frequency (IDF) curves, was adopted to obtain the synthetic hyetographs. The ABM considers storms of different possible combinations of intensity and duration for the same return period, which are largely associated with runoff (Ghazavi *et al.* 2017).

4. RESULTS

4.1. Defining sensitive parameters

As a rule of thumb, many parameters are defined in EPA-SWMM; however, it is worth mentioning that not all of those parameters need to be calibrated as some of them are insensitive compared to the others and changing their values during the automatic calibration process does not make a significant impact in the simulation results. For this reason, a sensitivity analysis was performed to evaluate the effect of the parameters defined in the EPA-SWMM model on simulation results. PEST was utilized to define the key parameters instead of the conventional trial-error method. First, the sensitivity results of PEST were obtained and then the sensitivity indices of EPA-SWMM parameters were normalized between zero and one. The sensitivity results showed that eight of the EPA-SWMM parameters have considerable effect on the model performance. Table 5 presents the normalized sensitivity NSE values of the eight EPA-SWMM parameters.

Table 5 reveals that the most sensitive parameter is *roughness*. Note that the roughness represents the roughness coefficient of channels and the storm water pipe network. Also, as can be seen from Table 5, the less influential parameter is the *maxrate*, which is introduced as the maximum infiltration rate on the Horton curve (Rossman 2015). Considering both the model efficiency and the computational cost, the abovementioned eight parameters were included in the model.

4.2. Model calibration and validation

EPA-SWMM does not contain an internal calibration option. Thus, an external calibration tool was considered to determine the optimum parameter values. In this direction, PEST was utilized for model calibration as the automatic calibration

Table 5 | Normalized (from 0 to 1) sensitivity indices of eight EPA SWMM parameters

Parameter name	Normalized sensitivity NSE
N-Imperv	0.092
N-Perv	0.046
pctzero	0.046
maxrate	0.016
minrate	0.065
decay	0.058
drytime	0.019
roughness	0.999

approaches in determining the optimized parameters significantly increase the modeling accuracy. The model calibration was performed based on the 12 multiple events occurred in the Ayamama watershed. The obtained time series for both the rainfall and the water depth are recorded at 1-min intervals (between January 2012 and December 2018). In this study, the 1-min interval rainfall data was aggregated to the 5-min interval and the 5-min average water depth values were calculated for the hydrograph estimation. We preferred to carry out the model calibration based on sequential multiple events rather than considering single event calibration. Therefore, the rainfall and water depth time series were constituted by aligning 12 different events data consecutively (Figure 4(a)). These sequential storm events were considered as an input for EPA-SWMM and the parameter optimization was done against the water depth time series data that correspond to those storm events. Also, the concentration time of the Ayamama watershed was taken into consideration to match the observed rainfall and water depth records.

Figure 4(a) shows the storm event hyetographs and hydrographs (in terms of water depth, cm) used for the model calibration. Note that the numbers in the brackets indicate the storm event numbers. On the one hand, the calibrated model

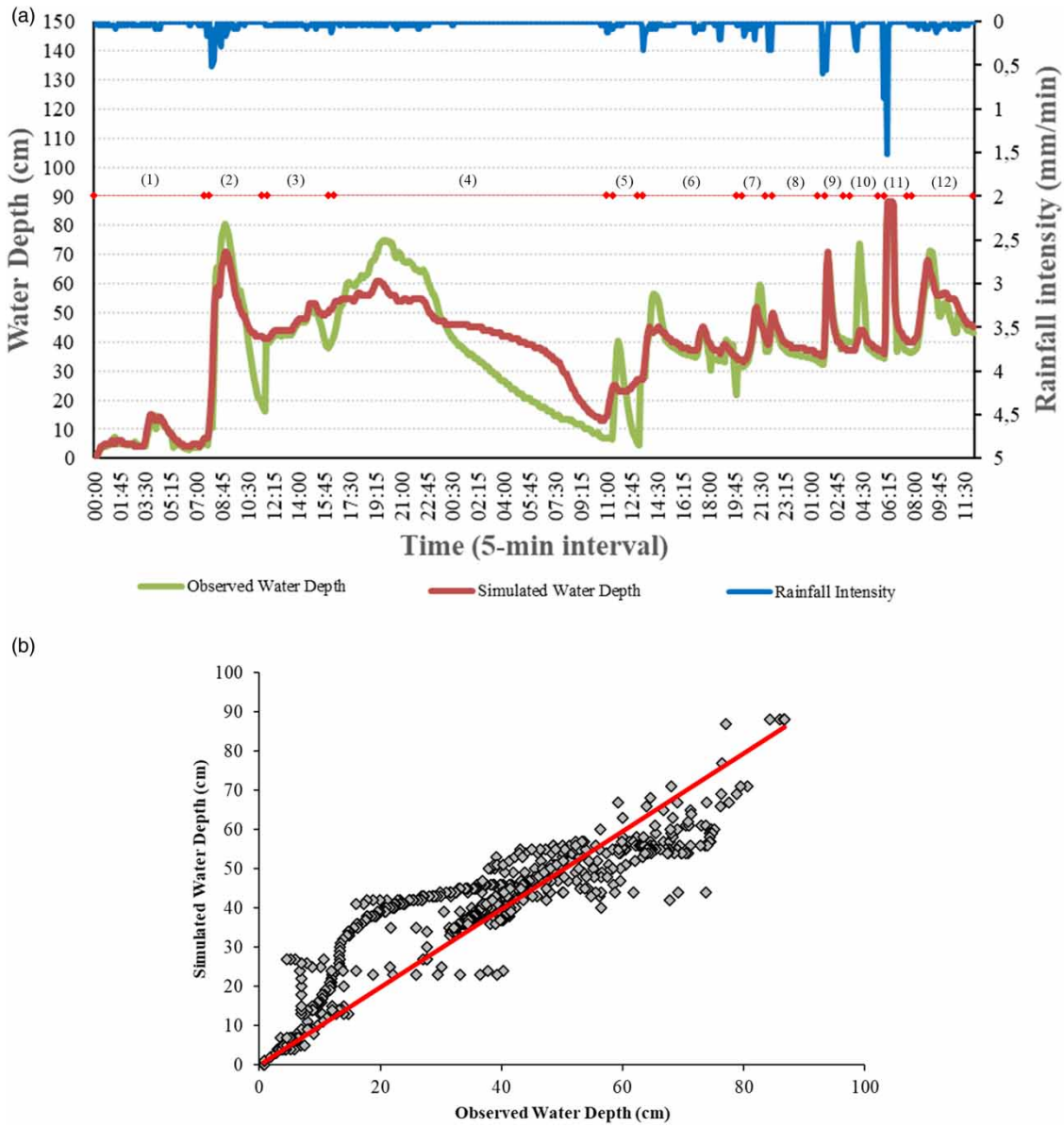

Figure 4 | The integrated PEST-SWMM calibration results, (a) consecutively combined 12 events' time series, (b) the scatter diagrams of the calibration results.

performs well particularly for most of the peak discharges as well as showing a good match in earlier and later events for the smaller discharges. On the other hand, the model has relatively lower accuracy for the events that have longer durations. In the model calibration, the NSE was chosen as the objective function. The NSE value was calculated as 0.809, which can be considered in a statistically acceptable range (NSE > 0.5) according to Moriasi *et al.* (2015). Also, Figure 4(b) shows that the model overestimates small discharge values, while it underestimates larger discharge values. In addition to the NSE, the calibration performance was evaluated against various performance indicators, as included in Table 6. The performance index (PI) and relative error (RE) were close to zero, while the Nash Sutcliffe efficiency coefficient (NSE) and Wilmott's refined index (WI) were close to one; such that those are the desired cases for the statistical evaluation of the hydrological models. To execute the models for calibration, we employed a Windows workstation with Intel(R) Core (TM) i5-7400 CPU (3.00 GHz and 8GB RAM).

As a result of the model calibration, the optimum values of the selected eight sensitive parameters were obtained and are presented in Table 7.

In addition to the model calibration, the validation of the PEST-SWMM model was conducted based on the storm events acquired through another meteorological-hydrological observation station; that is, the 212 Station, located on the Ayamama stream (Figure 1). In this context, four different storm events took place between 2019 and 2020 (two of them in 2019 and two of them in 2020) were collected. The validation was performed through the four consecutively arrayed storm events based on the calibrated sensitive parameters. According to the validation results, NSE was obtained as 0.624. The scatter diagram illustrating the simulated water depth vs observed flow depth is presented in Figure 5(a). The results showed that PEST-SWMM has considerable accuracy particularly for the observed flow depths below 35 cm. Above 35 cm, the validation results barely scattered against the observations. Also, the time series graph including both simulated and observed water depths for the validation period is presented in Figure 5(b). This figure highlights some significant differences between the PEST-SWMM results and observations, especially in extreme high water depths. This can be due to the fact that the acquired storms were identified as consecutive events. Overall, the auto-calibrated hydrological model; that is, PEST-SWMM, gave an acceptable performance for the validation as the NSE value is greater than 0.5 and the recorded water depths were well-captured except extreme highs.

4.3. Low impact development application

In this research, the required IDF curves were taken from the Turkish State Meteorological Service (MGM 2020). Considering the concentration time, which is related to several watershed characteristics such as the surface area and shape of the

Table 6 | PEST-SWMM calibration performance according to different performance indicators

	Performance Indicators				
	NSE	RMSE	PI	WI	RE
PEST-SWMM	0.809	33.304	0.479	0.799	0.279

Table 7 | Calibrated parameter values

Parameter name	Optimized value
N-Imperv	0.002
N-Perv	0.019
pctzero	9.999
maxrate	0.999
minrate	0.567
decay	2.001
drytime	8.007
roughness	0.041

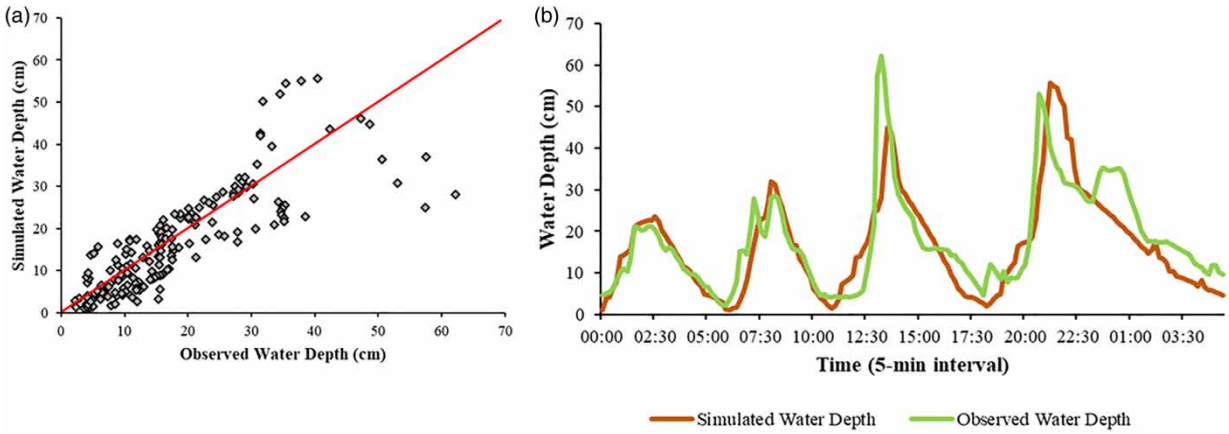

Figure 5 | The validation results of PEST-SWMM. (a) Scatter plot, (b) time series.

investigated site, duration of the synthetic storm events was determined as eight hours. In the light of these conditions, we applied the LID practices by means of the LID controls toolbox in the SWMM and the hydrograph estimation for each scenario was performed. Also, the combination scenario was determined according to the runoff reductions provided by the standalone LID techniques; such that the green roof and permeable pavements are two of the best performed practices. Figure 6 illustrates that the application of green roof leads to more decrease in peak discharge and runoff volume compared to the permeable pavement and bioretention cells. This pattern can be observed for each return period of a storm event. From Figure 6, it is apparent that the highest reduction of the peak discharge occurs for the combination of the green roof and the permeable pavements. For instance, the peak water depth was calculated as nearly 0.3 m in the case where LID was not considered for 2-year return period of a storm event. However, the peak water depth was reduced to 0.187 m, 0.178 m and 0.148 m for the permeable pavement, the green roof and the combination scenarios, respectively. Also, for the 100-year return period, the peak water depth was reduced from 0.90 m to 0.817, 0.80 m, 0.754 m and 0.589 m for the bioretention cells, permeable pavement, the green roof and the combination scenarios, respectively. No significant change is observed in the peak delay for each case. In addition, we present the peak runoff reduction and the volume reduction rates in Table 8.

It is obvious that the increasing storm event return period leads to an increase in peak discharge. However, the peak runoff reduction percentage decreases as the return period is increased. Among the return period scenarios, the lowest decrease in the peak runoff reduction exists for a 100-year return period with 15.68%, 10.28% and 34.51% for the green roof, the permeable pavement and the combination of them, respectively. It should also be noted that bioretention cells were not found as suitable for higher return period of storm events as they provide only 18.17% and 3.88% peak runoff reductions for 50 years and 100 years, respectively. On the other hand, we could not observe such a difference among the return periods of storm events in terms of volume reduction rates. Strong evidence of a maximum volume reduction was found in the combination scenario (green roof+permeable pavement). As can be seen from Table 8, the maximum volume reduction is calculated as 58.78% for the 10-year return period.

5. DISCUSSION

One of the main findings of the simulations showed that runoff reductions in terms of both average volume and peak volume of flows are decreased with the increasing storm event return periods. These results comply with the findings of other scholars, such as Locatelli *et al.* (2014), who found that green roofs provide nearly 50% peak reduction for 1-year return period while the peak reduction reduces to nearly 30% as the return period of the storm event increases to 10 years. In addition, Liu & Chui (2019) found similar findings for three different study areas as the peak runoff reduction decreases when the duration of the storm event increases. On the other hand, it can be stated that this is not always the case. For instance, in the same study of Liu & Chui (2019), they found that the amount of peak runoff increased through the increasing storm event return periods. This can be explained by the fact that peak reduction is highly dependent upon the available soil storage, formation of LID practices, as well as the rainfall characteristics of the selected study region.

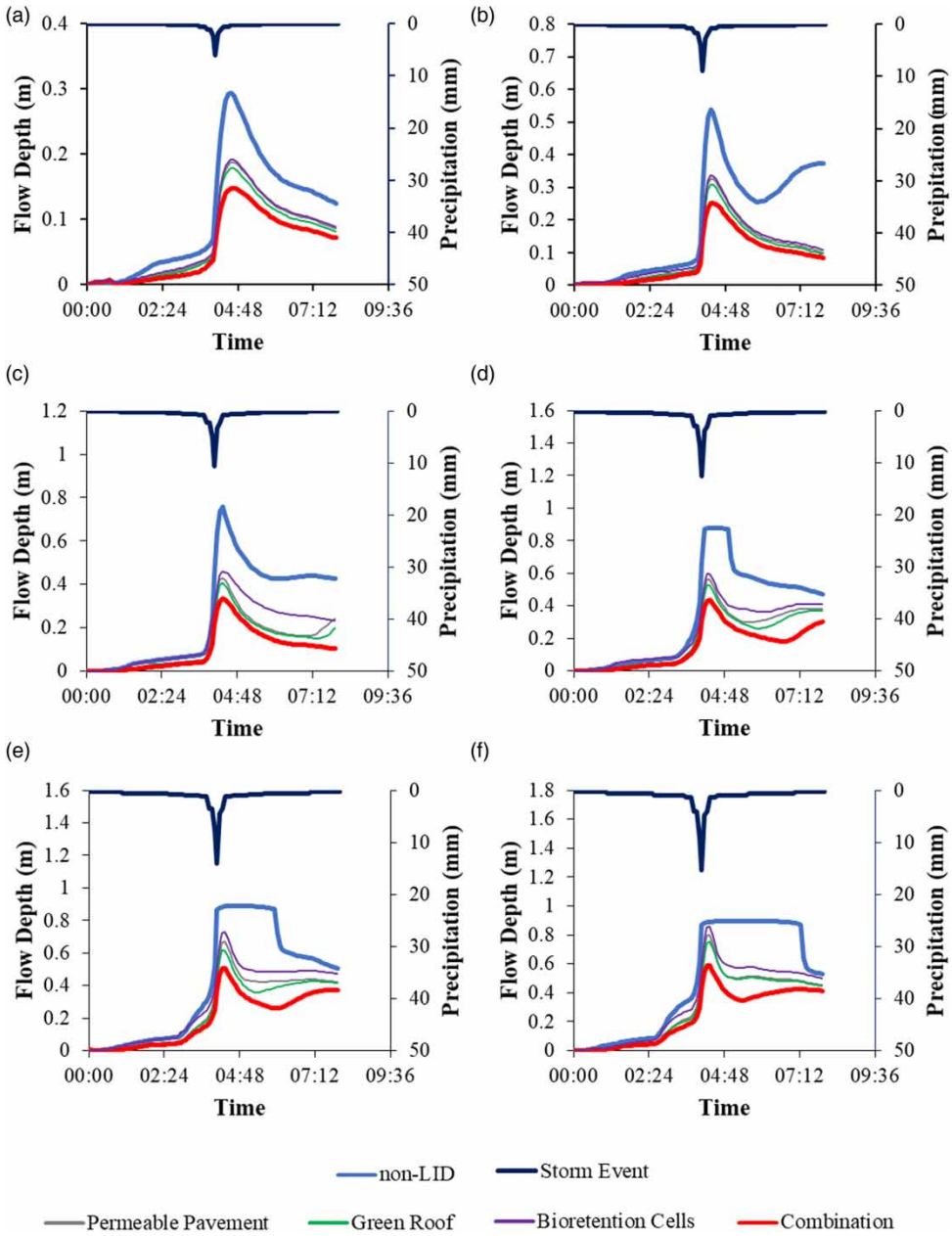

Figure 6 | Hydrograph estimations as a result of the LID techniques with respect to different return periods (a) 2-year, (b) 5-year, (c) 10-year, (d) 25-year, (e) 50-year, (f) 100-year.

The results of the LID practices are also in line with the pertinent literature; such that green roofs are shown as the feasible option among other LIDs by many scholars (Cristiano *et al.* 2020; Arjenaki *et al.* 2021). For instance, Arjenaki *et al.* (2021) found green roofs more advantageous than permeable pavements and rain barrels as the green roof provides the highest decrease rate in the volume and discharge peak of runoff. Also, other LIDs implemented within the scope of this study enable several benefits such that permeable pavements provide not only a significant reduction on cumulative runoff volumes but also considerable delay in the formation of peak flows (Tirpak *et al.* 2021) and bioretention cells have an important function in the reduction of magnitude of the flow and the degree of groundwater recharge (Sun *et al.* 2019). Despite the aforementioned pros of these LIDs, the performance of the adopted LID methodology is highly related to the coverage area (Roseen *et al.* 2012). Thus, the difference between both the runoff volume reduction and peak runoff reduction for

Table 8 | The peak runoff reduction and the volume reduction rates with respect to different return periods

		Return period (Year)					
		2	5	10	25	50	100
Peak Runoff Reduction (%)	Green poof	39.36	43.14	46.49	40.45	30.25	15.68
	Permeable pavement	36.27	39.83	43.27	36.29	24.53	10.28
	Bioretention cells	34.84	37.80	39.56	32.30	18.17	3.88
	Combination	49.66	53.19	56.02	50.49	42.86	34.51
Volume Reduction (%)	Green roof	39.42	46.34	48.07	40.98	39.94	39.69
	Permeable pavement	35.81	45.82	44.59	37.04	36.25	37.18
	Bioretention cells	32.18	36.62	37.38	30.29	28.26	27.73
	Combination	48.30	53.20	58.79	54.35	50.37	50.84

green roof and permeable pavement may be explained with the area covered by the green roof in this study (8.90%) being larger than the permeable pavement (6.85%). The difference between the selected coverage areas comes from the fact that each LID form could be determined considering the local conditions of the study area (Yazdi & Salehi Neyshabouri 2014). Also, the performance of the bioretention cells was lower compared to green roofs even though the covered practicing areas were almost similar to each other (8.1% of the total watershed area for bioretention cells). This is contrary to the findings of DeBusk & Wynn (2011), in which greater than 97% volume reduction was obtained by them when the bioretention cells were applied to parking lots. Overall, the findings of this study showed that bioretention was not a feasible alternative for the highly urbanized Ayamama watershed based on the peak runoff and volume reduction values presented in Table 8. It is therefore the bioretention cells were not included in the combination scenario.

Furthermore, specific to the Ayamama watershed, the results showed that the water depth significantly increases particularly for 25, 50 and 100-year return periods of storm events when the LID practices were not considered. Even tough LID designs are more beneficial for relatively low recurrence intervals, such as 2, 5 and 10 years (Fassman & Blackbourn 2010; Liao *et al.* 2014), in terms of the management of water quantity (Czemiel Berndtsson 2010), two of the implemented LID techniques in this study; that is, green roof and permeable pavements, well-performed for higher recurrence intervals in terms of both peak runoff and volume reductions as these are the most effective criteria in the evaluation of LID performances (Ahiablame & Shakya 2016; Koc *et al.* 2021). Overall, the results revealed that the impact of a possible storm event that could have serious consequences in the highly urbanized Ayamama watershed can be reduced with the implementation of the combination of green roofs and permeable pavements.

6. CONCLUSIONS

This paper was designed to determine the impacts of the up-to-date LID practices on off-site runoff mitigation performance for sustainable water resources management strategies. In this regard, LID controls were applied for providing an environmental sensitive planning to the highly urbanized Ayamama watershed of Istanbul, Turkey. The most commonly used LID techniques, i.e. green roof, permeable pavements and bioretention cells, and the combination of the two best-performing LIDs were applied to reduce the surface runoff in Ayamama watershed. Since the watershed is densely populated and highly urbanized in recent years, applying LID techniques was preferred rather than the conventional flood mitigation strategies to reduce the peak flow along with providing an aesthetic appearance. Moreover, the well-known PEST optimization tool was integrated with the EPA-SWMM hydrologic-hydraulic model for not only obviating uncertainties by sensitivity analysis but also for defining the optimum values of the sensitive parameters by means of the model calibration. The PEST-SWMM model was calibrated and validated against the sequential multiple events that were obtained from the 1-min interval rainfall and water depth measurements. The NSE was used as the single objective function for the auto-calibrated model. Then, the LID practices were applied to the auto-calibrated PEST-SWMM to investigate the peak runoff reduction and the volume reduction rates. The ABM was used for the synthetic storm event hyetographs considering the six return periods, i.e. 2, 5, 10, 25, 50 and 100 years. The following conclusions can be drawn from the present study:

1. The PEST software can be used for the auto-calibration of SWMM and the objective function, NSE, is calculated as 0.81. The calibration results were statistically significant according to the various performance indicators.

2. Among the single LIDs, the green roof application has more impact on both the peak discharge reduction and the volume reduction than the permeable pavements and bioretention cells for each storm event scenario that has different return periods.
3. The application of bioretention was not found to be feasible to reduce the peak runoff when the higher return period of storm events; that is, 50 years and 100 years, were considered.
4. Although the green roof, permeable pavements and bioretention cells made significant contribution to the surface runoff mitigation, the combination scenario (green roof+permeable pavement) had superior effect than the single LID applications.
5. In general, the peak runoff reduction tends to decrease as return periods increase. However, we did not observe a considerable variation in the percentage of volume reductions with respect to the return periods.
6. The maximum peak runoff reduction was observed in a 10-year return period of a storm event in standalone LIDs and combination scenario.

In the light of the abovementioned key findings, a robust auto-calibrated PEST-SWMM model was proposed. We also presented that the combination of the green roof and the permeable pavements leads to a serious increase in both surface peak runoff reduction and the volume reductions for highly urbanized watersheds.

An issue that was not addressed in this study is whether any option to optimize the LID control parameters exists or not. The impact of the multiple objective function on the model calibration should be considered in the future work. In addition, considerably more work will need to be done to establish a comprehensive framework, which consists of the economic, environmental and social effects of the LID strategies. Notwithstanding these limitations, the evaluation of possible LID controls was presented to mitigate the urban floods in densely populated areas. Furthermore, this study consists of useful outcomes for decision-makers, water resource professionals and local authorities to develop flood risk mitigation strategies.

ACKNOWLEDGEMENTS

The authors would like to express their gratitude to the Istanbul Water and Sewerage Administration (ISKI), Istanbul Metropolitan Municipality Disaster Coordination Center (AKOM) and Turkish State Meteorological Service (MGM) for their support.

DATA AVAILABILITY STATEMENT

Data cannot be made publicly available; readers should contact the corresponding author for details.

REFERENCES

Abi Aad, M. P., Suidan, M. T. & Shuster, W. D. 2010 Modeling techniques of best management practices: rain barrels and rain gardens using EPA SWMM-5. *Journal of Hydrologic Engineering* **15** (6), 434–443.

Abualfaraj, N., Cataldo, J., Elborolosy, Y., Fagan, D., Woerdeman, S., Carson, T. & Montalto, F. A. 2018 Monitoring and modeling the long-term rainfall-runoff response of the Jacob K. Javits Center green roof. *Water (Switzerland)* **10** (11), 1–23.

Ahiablame, L. & Shakya, R. 2016 Modeling flood reduction effects of low impact development at a watershed scale. *Journal of Environmental Management* **171**, 81–91.

Ahmed, K., Chung, E. S., Song, J. Y. & Shahid, S. 2017 Effective design and planning specification of low impact development practices using Water Management Analysis Module (WMAM): case of Malaysia. *Water (Switzerland)* **9** (3), 173.

AKOM 2020 Preparation and planning.

Arjenaki, M. O., Sanayei, H. R. Z., Heidarzadeh, H. & Mahabadi, N. A. 2021 Modeling and investigating the effect of the LID methods on collection network of urban runoff using the SWMM model (case study: Shahrekord City). *Modeling Earth Systems and Environment* **7** (1), 1–16.

Bai, Y., Zhao, N., Zhang, R. & Zeng, X. 2018 Storm water management of low impact development in urban areas based on SWMM. *Water (Switzerland)* **11** (1), 33.

BIMTAS 2020 *Analytical Surveys of Istanbul Project*. Available from: https://bimtas.istanbul..

Biondi, D., Freni, G., Iacobellis, V., Mascaro, G. & Montanari, A. 2012 'Validation of hydrological models: conceptual basis, methodological approaches and a proposal for a code of practice. *Physics and Chemistry of the Earth* **42–44**, 70–76.

Burszta-Adamiak, E. & Mrowiec, M. 2013 Modelling of green roofs' hydrologic performance using EPA's SWMM. *Water Science and Technology* **68**, 36–42.

Cano, O. M. & Barkdoll, B. D. 2017 Multiobjective, socioeconomic, boundary-emanating, nearest distance algorithm for stormwater low-impact BMP selection and placement. *Journal of Water Resources Planning and Management* **143** (1), 1–9.

Chung, E. S., Hong, W. P., Lee, K. S. & Burian, S. J. 2011 Integrated use of a continuous simulation model and multi-attribute decision-making for ranking urban watershed management alternatives. *Water Resources Management* **25** (2), 641–659.

Copernicus Europe's Eye on Earth and Land Monitoring Service 2020 *CORINE Land Cover Data*. Available from: https://land.copernicus.eu.

Cristiano, E., Urru, S., Farris, S., Ruggiu, D., Deidda, R. & Viola, F. 2020 Analysis of potential benefits on flood mitigation of a CAM green roof in Mediterranean urban areas. *Building and Environment* **183**, 107179.

Cristiano, E., Farris, S., Deidda, R. & Viola, F. 2021 Comparison of blue-green solutions for urban flood mitigation: a multi-city large-scale analysis. *PLOS ONE, (A. Zanini, ed.)* **16** (1), e0246429.

Czemiel Berndtsson, J. 2010 Green roof performance towards management of runoff water quantity and quality: a review. *Ecological Engineering* **36** (4), 351–360.

DeBusk, K. M. & Wynn, T. M. 2011 Storm-water bioretention for runoff quality and quantity mitigation. *Journal of Environmental Engineering* **137** (9), 800–808.

Demuzere, M., Orru, K., Heidrich, O., Olazabal, E., Geneletti, D., Orru, H., Bhave, A. G., Mittal, N., Feliu, E. & Faehnle, M. 2014 Mitigating and adapting to climate change: multi-functional and multi-scale assessment of green urban infrastructure. *Journal of Environmental Management* **146**, 107–115.

Doherty, J. 2018 PEST Model-Independent Parameter Estimation User Manual Part I: PEST, SENSAN and Global Optimisers Watermark Numerical Computing Acknowledgements. 393.

Eckart, K., McPhee, Z. & Bolisetti, T. 2018 Multiobjective optimization of low impact development stormwater controls. *Journal of Hydrology* **562**, 564–576.

Ekmekcioğlu, Ö., Koc, K. & Özger, M. 2020 District based flood risk assessment in Istanbul using fuzzy analytical hierarchy process. *Stochastic Environmental Research and Risk Assessment* **35**, 617–637.

Ekmekcioğlu, Ö., Koc, K. & Özger, M. 2021 Stakeholder perceptions in flood risk assessment: a hybrid fuzzy AHP-TOPSIS approach for Istanbul, Turkey. *International Journal of Disaster Risk Reduction* **60**, 102327.

Fassman, E. A. & Blackbourn, S. 2010 Urban runoff mitigation by a permeable pavement system over impermeable soils. *Journal of Hydrologic Engineering* **15** (6), 475–485.

Gandomi, A. H. & Roke, D. A. 2015 Assessment of artificial neural network and genetic programming as predictive tools. Advances in Engineering S*oftware* **88**, 63–72.

Ghazavi, R., Rabori, A. M. & Reveshty, M. A. 2017 The effects of rainfall intensity-duration-frequency curves reformation on urban flood characteristics in semi-arid environment. *Ecopersia* **5** (2), 1799–1813.

Guan, M., Sillanpää, N. & Koivusalo, H. 2015 Modelling and assessment of hydrological changes in a developing urban catchment. *Hydrological Processes* **29** (13), 2880–2894.

Gülbaz, S. & Kazezyılmaz-Alhan, C. M. 2017 Hydrological model of LID with rainfall-watershed-bioretention system. *Water Resources Management* **31** (6), 1931–1946.

Gülbaz, S., Kazezyilmaz-Alhan, C. M., Bahçeçi, A. & Boyraz, U. 2019 Flood modeling of Ayamama river watershed in Istanbul, Turkey. *Journal of Hydrologic Engineering* **24**, 1.

Hamouz, V. & Muthanna, T. M. 2019 Hydrological modelling of green and grey roofs in cold climate with the SWMM model. *Journal of Environmental Management* **249**, 109350.

Hossain, S., Hewa, G. A. & Wella-Hewage, S. 2019 A comparison of continuous and event-based rainfall-runoff (RR) modelling using EPA-SWMM. *Water (Switzerland)* **11** (3), 611.

Houdeshel, C. D., Pomeroy, C. A. & Hultine, K. R. 2012 Bioretention design for Xeric climates based on ecological principles. *JAWRA Journal of the American Water Resources Association* **48** (6), 1178–1190.

Istanbul Water and Sewerage Administration (ISKI) 2020 *Digital Terrain Elevation Data*. Available from: https://www.iski.istanbul/web..

Koc, K. & Işık, Z. 2020 A multi-agent-based model for sustainable governance of urban flood risk mitigation measures. *Natural Hazards* **104** (1), 1079–1110.

Koc, K., Ekmekcioğlu, Ö. & Özger, M. 2021 An integrated framework for the comprehensive evaluation of low impact development strategies. *Journal of Environmental Management* **294**, 113023.

Krebs, G., Kokkonen, T., Valtanen, M., Koivusalo, H. & Setälä, H. 2013 A high resolution application of a stormwater management model (SWMM) using genetic parameter optimization. *Urban Water Journal* **10** (6), 394–410.

Li, J., Li, Y. & Li, Y. 2016 SWMM-based evaluation of the effect of rain gardens on urbanized areas. *Environmental Earth Sciences* **75** (1), 1–14.

Liao, Z., Chen, H., Huang, F. & Li, H. 2014 Cost–effectiveness analysis on LID measures of a highly urbanized area. *Desalination and Water Treatment* **56** (11), 1–7.

Liew, Y. S., Mat Desa, S., Noh, M., Nasir, M., Tan, M. L., Zakaria, N. A. & Chang, C. K. 2021 Assessing the effectiveness of mitigation strategies for flood risk reduction in the Segamat river basin, Malaysia. *Sustainability* **13** (6), 3286.

Liu, Y. B., Batelaan, O., De Smedt, F., Poórová, J. & Velcická, L. 2005 Automated calibration applied to a GIS-based flood simulation model using PEST. In: *Floods, From Defence to Management* (van Alphen, J., van Beek, E. & Taal, M., eds.). Taylor & Francis, London, 317–326.

Liu, Y. & Gupta, H. V. 2007 Uncertainty in hydrologic modeling: toward an integrated data assimilation framework. *Water Resources Research* **43** (7), 1–18.

Liu, R. & Fassman-Beck, E. 2017 Hydrologic response of engineered media in living roofs and bioretention to large rainfalls: experiments and modeling. *Hydrological Processes* **31** (3), 556–572.
Liu, X. & Chui, T. F. M. 2019 Evaluation of Green roof performance in mitigating the impact of extreme storms. *Water* **11** (4), 815.
Locatelli, L., Mark, O., Mikkelsen, P. S., Arnbjerg-Nielsen, K., Bergen Jensen, M. & Binning, P. J. 2014 Modelling of green roof hydrological performance for urban drainage applications. *Journal of Hydrology* **519**, 3237–3248.
Masseroni, D. & Cislaghi, A. 2016 Green roof benefits for reducing flood risk at the catchment scale. *Environmental Earth Sciences* **75**, 7.
Men, H., Lu, H., Jiang, W. & Xu, D. 2020 Mathematical optimization method of low-impact development layout in the Sponge city. *Mathematical Problems in Engineering* **2020**, 1–17.
MGM 2020 Statistics. Available from: https://www.mgm.gov.tr
Moriasi, D. N., Gitau, M. W., Pai, N. & Daggupati, P. 2015 Hydrologic and water quality models: performance measures and evaluation criteria. *Transactions of the ASABE* **58** (6), 1763–1785.
Nash, J. E. & Sutcliffe, J. V. 1970 River flow forecasting through conceptual models. Part 1: a discussion of principles. *Journal of Hydrology* **10** (3), 282–290.
Nigussie, T. A. & Altunkaynak, A. 2016 Assessing the hydrological response of Ayamama watershed from urbanization predicted under various landuse policy scenarios. *Water Resources Management* **30** (10), 3427–3441.
Palla, A. & Gnecco, I. 2015 Hydrologic modeling of Low impact development systems at the urban catchment scale. *Journal of Hydrology* **528**, 361–368.
Peng, Z. & Stovin, V. 2017 Independent validation of the SWMM green roof module. *Journal of Hydrologic Engineering* **22** (9), 1–12.
Perin, R., Trigatti, M., Nicolini, M., Campolo, M. & Goi, D. 2020 Automated calibration of the EPA-SWMM model for a small suburban catchment using PEST: a case study. *Environmental Monitoring and Assessment* **192**, 6.
PEST n.d. *Parameter ESTimation Tool (PEST)*. Available from: http://www.pesthomepage.org.
Platz, M., Simon, M. & Tryby, M. 2020 Testing of the storm water management model Low impact development modules. *Journal of the American Water Resources Association* **56** (2), 283–296.
Qin, H. P., Li, Z. X. & Fu, G. 2013 The effects of low impact development on urban flooding under different rainfall characteristics. *Journal of Environmental Management* **129**, 577–585.
Rodrigues, A. L. M., da Silva, D. D. & de Menezes Filho, F. C. M. 2021 Methodology for allocation of best management practices integrated with the urban landscape. *Water Resources Management* **35** (4), 1353–1371.
Roseen, R. M., Ballestero, T. P., Houle, J. J., Briggs, J. F. & Houle, K. M. 2012 Water quality and hydrologic performance of a porous asphalt pavement as a storm-water treatment strategy in a cold climate. *Journal of Environmental Engineering* **138** (1), 81–89.
Rossman, L. A. 2015 *Storm Water Management Model User's Manual Version 5.1*. U.S. Environmental Protection Agency, Cincinnati, OH.
Rycewicz-Borecki, M., McLean, J. E. & Dupont, R. R. 2017 Nitrogen and phosphorus mass balance, retention and uptake in six plant species grown in stormwater bioretention microcosms. *Ecological Engineering* **99**, 409–416.
Shahed Behrouz, M., Zhu, Z., Matott, L. S. & Rabideau, A. J. 2020 A new tool for automatic calibration of the storm water management model (SWMM). *Journal of Hydrology* **581**, 124436.
Sun, Y., Pomeroy, C., Li, Q. & Xu, C. 2019 Impacts of rainfall and catchment characteristics on bioretention cell performance. *Water Science and Engineering* **12** (2), 98–107.
Taji, S. G. & Regulwar, D. G. 2019 LID coupled design of drainage model using GIS and SWMM. *ISH Journal of Hydraulic Engineering*, 1–14.
Tirpak, R. A., Winston, R. J., Simpson, I. M., Dorsey, J. D., Grimm, A. G., Pieschek, R. L., Petrovskis, E. A. & Carpenter, D. D. 2021 Hydrologic impacts of retrofitted low impact development in a commercial parking lot. *Journal of Hydrology* **592**, 125773.
Willmott, C. J., Robeson, S. M. & Matsuura, K. 2012 A refined index of model performance. *International Journal of Climatology* **32** (13), 2088–2094.
Yazdi, J. & Salehi Neyshabouri, S. A. A. 2014 Identifying low impact development strategies for flood mitigation using a fuzzy-probabilistic approach. *Environmental Modelling & Software* **60**, 31–44.
Yin, D., Evans, B., Wang, Q., Chen, Z., Jia, H., Chen, A. S., Fu, G., Ahmad, S. & Leng, L. 2020 Integrated 1D and 2D model for better assessing runoff quantity control of low impact development facilities on community scale. *Science of The Total Environment* **720**, 137630.
Zhang, S. & Guo, Y. 2014 Stormwater capture efficiency of bioretention systems. *Water Resources Management* **28** (1), 149–168.
Zhang, K., Chui, T. F. M. & Yang, Y. 2018 Simulating the hydrological performance of low impact development in shallow groundwater via a modified SWMM. *Journal of Hydrology* **566**, 313–331.

First received 15 May 2021; accepted in revised form 17 September 2021. Available online 30 September 2021